

NASA TECHNICAL  
MEMORANDUM



NASA TM X-1205

NASA TM X-1205



STATIC AND DYNAMIC  
CHARACTERISTICS OF  
CENTAUR GIMBAL SYSTEM  
UNDER THRUST LOAD

*by Robert J. Antl, David W. Vincent, and Larry D. Pleuss*

*Lewis Research Center  
Cleveland, Ohio*





STATIC AND DYNAMIC CHARACTERISTICS OF CENTAUR  
GIMBAL SYSTEM UNDER THRUST LOAD

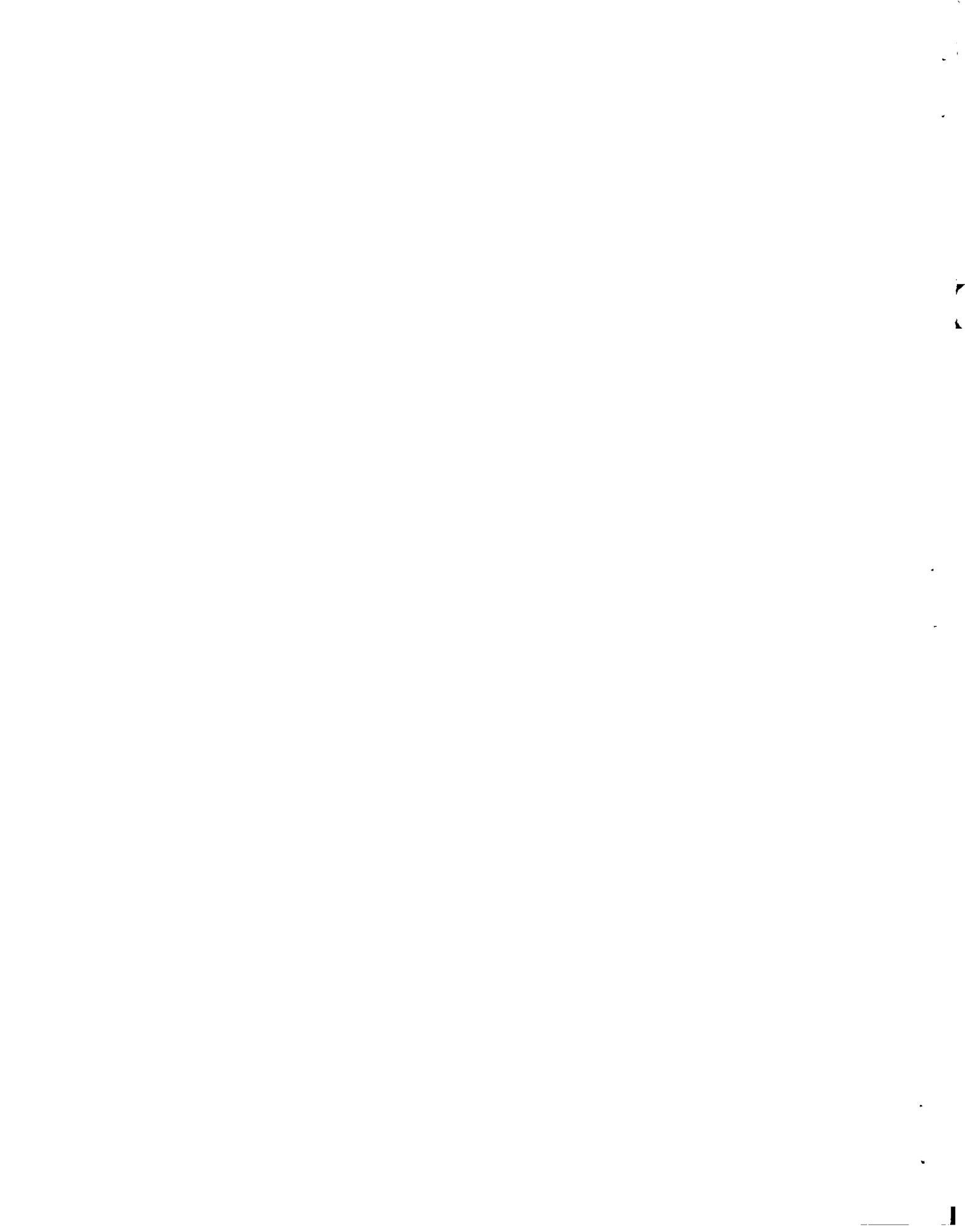
By Robert J. Antl, David W. Vincent, and Larry D. Plews

Lewis Research Center  
Cleveland, Ohio

NATIONAL AERONAUTICS AND SPACE ADMINISTRATION

---

For sale by the Clearinghouse for Federal Scientific and Technical Information  
Springfield, Virginia 22151 - Price \$1.00



## STATIC AND DYNAMIC CHARACTERISTICS OF CENTAUR

### GIMBAL SYSTEM UNDER THRUST LOAD

by Robert J. Antl, David W. Vincent, and Larry D. Flews

Lewis Research Center

#### SUMMARY

Tests to determine the static and dynamic characteristics of the Centaur gimbal system under thrust load were conducted in an altitude facility of the Lewis Research Center. Included in the gimbal system were (1) a hydrogen-oxygen, regeneratively cooled RL10A-3 flight model engine and (2) Centaur actuators and hydraulic system. The purposes of these tests were to facilitate analyses of the system and to provide a basis for comparison with flight information.

The major objectives of the test program were (1) to determine the coulomb and viscous friction of the engine gimbal block, (2) to determine the frequency response of the system, and (3) to demonstrate the structural integrity of the system under dynamic stresses. Other constants needed to evaluate the system characteristics properly for the particular test setup were also determined. Included were the gravitational effects due to horizontal mounting of the engine, the thrust offset or misalignment vector of the engine, the facility propellant duct restraints, the transient response of the system, and the torsional loading of the gimbal block during slow movements, step changes, and cycling operation. The procedures used are outlined and the data obtained are presented in tabular and in graphical form.

#### INTRODUCTION

The use of a main engine gimbal system is one method used for vehicle stabilization, flight trajectory control after booster separation, or space docking maneuvers. Such a system is incorporated in the present Centaur upper-stage vehicle. The gimbal system consists of a hydraulic power unit directly coupled to the main engine power train and two servocontrolled actuators.

Tests to determine the characteristics of the Centaur gimbal system under thrust load and in an altitude environment were needed in order to provide information for analyses of both present and future systems. Such tests were undertaken at Lewis. The results of these tests are applicable to the present Centaur flight gimbal system; however, the procedures used for determining the various gimbal characteristics can be applied to future test programs.

A specific purpose of these tests was to determine the effect of thrust on the Centaur gimbal system static and dynamic capability and thus to facilitate analyses of the system and to provide a basis for comparison with flight data. The major objectives of the test program were threefold. One objective was to determine the coulomb and viscous friction of the engine gimbal block pins. In order to evaluate the data properly for analyses, other factors, such as the facility propellant duct restraints, the gravitational effects of mounting the engine horizontally, and the thrust offset or misalignment vector, were also determined. Another objective was to determine the frequency response of the gimbal system. The transient response, which includes the damping characteristics and the evaluation of times for 63.2 and 90 percent of change, was also determined. The third major objective was to demonstrate the structural integrity of the gimbal system under dynamic stresses. As part of this objective, factors concerned with the torsional load created by the offset center of mass of the engine were evaluated for transient operation. Included were slow movements, step changes, and cycling operation.

The engine used for the tests was a Pratt & Whitney RL10A-3 flight model, which is a hydrogen-oxygen, regeneratively cooled, pump-fed rocket engine. Performance characteristics of the engine are not presented herein; however, such information can be obtained from studies reported in references 1 and 2. The gimbal actuators and the hydraulic system were flight articles and were supplied by the Centaur vehicle manufacturer.

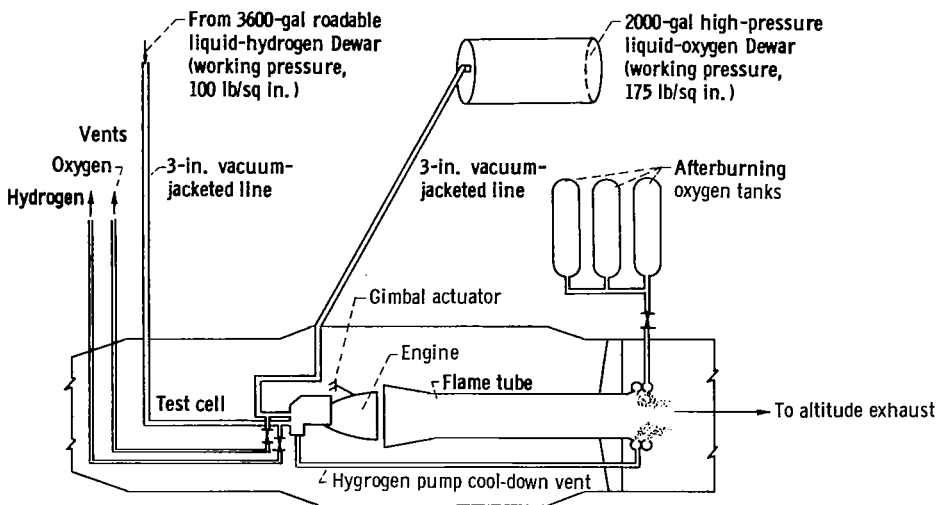
The investigation was conducted in an altitude facility which was capable of maintaining the altitude pressures required to provide full flow expansion in the nozzle. Procedures used are described, and the data obtained are presented in tabular and in graphical form.

## APPARATUS

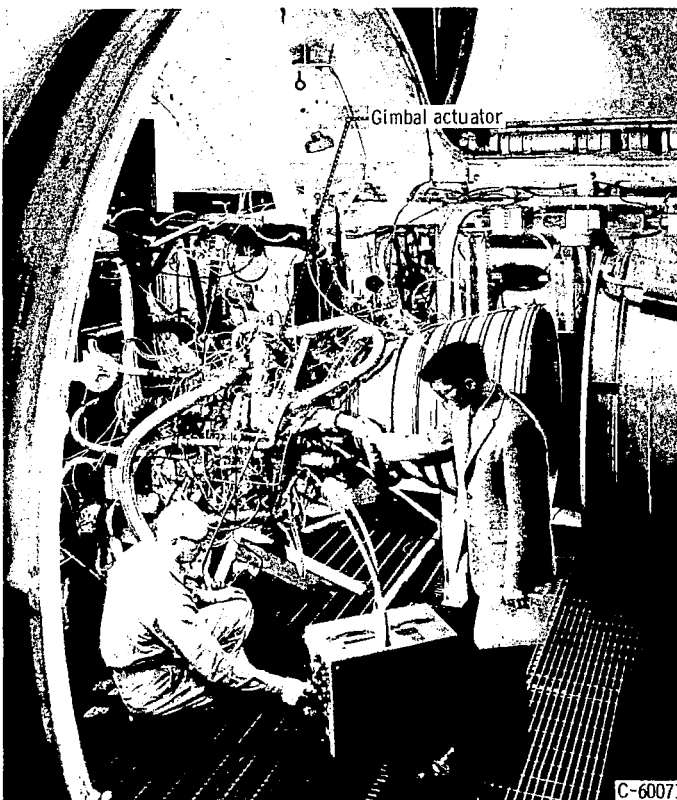
### Facility and Engine

The tests were conducted in a Lewis altitude chamber. A schematic diagram and a photograph of the test installation are presented in figure 1. Propellants were transferred with a conventional cryogenic pressurized system from Dewars located in the storage area through vacuum-jacketed lines. The facility exhaust system was capable of maintaining the required altitude pressures for full flow expansion in the rocket engine nozzle. An afterburner system added a sufficient quantity of oxygen to the rocket exhaust in order to burn any residual combustibles to completion. Data for the required amount of oxidant were obtained from studies reported in reference 3.

The engine used for the tests was a Pratt & Whitney RL10A-3 flight model (fig. 1(b)). At rated conditions, a chamber pressure of 300 pounds per square inch absolute and a propellant mixture ratio of 5.0, this engine produced 15 000 pounds of thrust in a vacuum environment. Details of the engine and components can be found in references 4 and 5. The engine was mounted horizontally in the test chamber, and a three-point suspension system, consisting of



(a) Schematic diagram of test chamber.



(b) Engine mounted in test stand.

Figure 1. - Test installation.

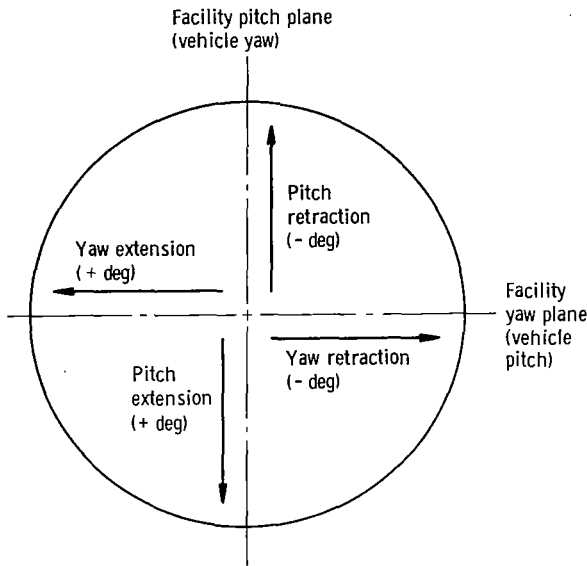


Figure 2. - Definition of actuator movements (viewed upstream).

the RL10 gimbal block mount and two gimbal actuators supplied by the Centaur vehicle manufacturer, was used to support the engine. Relative actuator movements, as viewed upstream, are defined in figure 2. The engine axes, as mounted in the test facility, were rotated  $90^\circ$  to those of the Centaur vehicle, and the data presented herein are based on the facility mounting. Since the existing thrust stand was used for the tests, Centaur spring constants were not simulated.

The Centaur flight gimbal system, supplied by the vehicle manufacturer, is a closed loop servocontrol system with its main component being the power package assembly and two servocontrolled actuators. The power package contains a miniature constant displacement, vane-type pump, which supplies flow at 1100

pounds per square inch gage pressure to the actuators, and is directly coupled to the engine oxygen pump drive. This pump functions only when the engine is firing. During flight coast periods, a thermostatically controlled, electrically operated pump circulates the hydraulic fluid through the system. Whenever the temperature in the hydraulic system falls below a predetermined value, the circulating pump is activated, and the entire system is maintained at a nearly uniform temperature. The circulating pump is also used for slow movements prior to engine start. In addition to the two vane pumps, the power package houses the necessary relief and check valves, an accumulator to dampen output pressure surges, and a reservoir to prevent cavitation of the main pump. The actuators are of trail-rod design to allow equal force to be exerted while the rod is retracted or extended.

A variable-displacement hydraulic pump was used during these tests to augment the Centaur system in providing the capability to hold the engine horizontal and for nonfiring operation. A complete description of the Centaur hydraulic system can be found in reference 6.

### Instrumentation

The engine was instrumented to monitor and record the engine operating parameters. Included among these were propellant flow rates, engine component inlet and outlet pressures and temperatures, combustion-chamber pressure, thrust, and ambient conditions. Pressure measurements were obtained by the use of strain-gage type transducers, and temperatures were measured by platinum resistance-type sensors (ref. 7).

Special instrumentation concerned with the gimbal system was also provided.

TABLE I. - GIMBAL INSTRUMENTATION

Description	Recorder
Actuator differential pressure	
Pitch	
High pressure	Digital and oscillograph
Low pressure	Oscillograph
Yaw	
High pressure	Digital and oscillograph
Low pressure	Oscillograph
Hydraulic oil pressure	Oscillograph
Hydraulic oil temperature 1	Digital
Hydraulic oil temperature 2	Digital
Gimbal bearing temperature	
Pitch	Digital
Yaw	Digital
Position indicators	
Engine position signal (linear potentiometer)	
Yaw	
Engine position 1 (64.49 in.) <sup>a</sup>	Digital and oscillograph
Engine position 2 (50.42 in.)	Digital and oscillograph
Engine position 3 (32.64 in.)	Digital and oscillograph
Pitch	
Engine position 1 (64.44 in.)	Digital and oscillograph
Engine position 2 (50.38 in.)	Digital and oscillograph
Engine position 3 (32.59 in.)	Digital and oscillograph
Input signal	
Pitch	Oscillograph
Yaw	Oscillograph
Feedback signal	
Pitch	Oscillograph
Yaw	Digital and Oscillograph
Gimbal angle (gimbal block), Yaw	Oscillograph
Torsional load	Digital and oscillograph

<sup>a</sup>Position measured axially from gimbal pin.

The gimbal instrumentation consisted of hydraulic oil pressure and temperature, actuator differential pressures, gimbal system input and feedback signals, and three linear potentiometers each for yaw and pitch mounted in the axial plane along the thrust chamber and nozzle skirt.

The parameters were recorded on an automatic digital data recorder capable of recording 4000 samples per second and on direct-writing oscillographs located in the facility control room. Transient and frequency response data were obtained from the oscillographs. Measured pressures were not corrected for the added dynamics of the connecting line lengths, whereas electrical signals (input and feedback signals) had no attenuation in the frequency range of interest. The gimbal instrumentation and the types of recorder used are listed in table I.

## PROCEDURE

### Engine Movements

Engine position was controlled by a servoamplifier system supplied by the

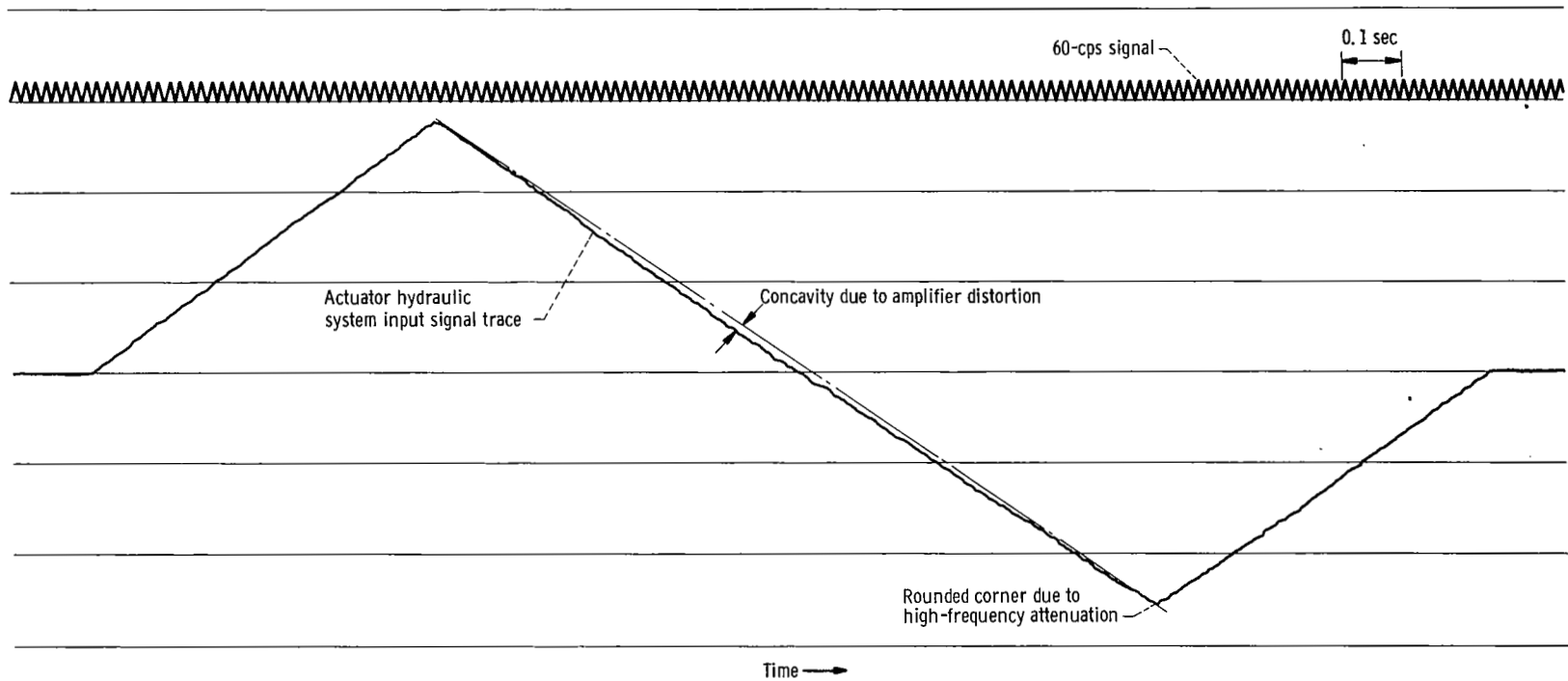


Figure 3. - Copy of typical oscillograph record showing nonlinearity of signal from servoamplifier.

vehicle manufacturer. The input signals for triangular and sinusoidal wave patterns were supplied by a low-frequency function generator and were stored on a magnetic-tape recorder. These input command signals were sent to the servo-amplifier, which operated the actuator piston, and to a direct-writing oscillograph. Presented in figure 3 is a copy of a typical oscillograph record showing the nonlinearity of the output signal from the servoamplifier which represents the input signal to the gimbal actuator hydraulic system. This figure depicts the distortion contributed by the servoamplifier, indicated by the concavity of the actuator input signal trace, and the high-frequency attenuation, indicated by the slightly rounded corners. The experimental data presented herein were based on the actuator input signal as shown in figure 3. Both the magnetic-tape handler and the step-function circuit were controlled by a motor-driven cam-type timer. The timer, which was accurate to 0.1 second, was started manually.

Feedback transducer calibrations, which determined the output of the feedback transducer in volts per degree of engine displacement, were made prior to testing. The procedures (engine movement patterns) used for the various tests are described in the RESULTS AND DISCUSSION.

#### Test Conditions

Prior to an engine firing, the facility propellant lines were cooled to ensure that liquid rather than gaseous propellants would be supplied to the engine pump inlets at the start. Proper altitude conditions were also set and maintained. The data presented are based on a test chamber pressure of approximately 0.25 pound per square inch absolute, which corresponds to an altitude of more than 90 000 feet.

After ambient conditions were set, an automatic time sequencing system was employed to control the events of the rocket engine start. When the engine was considered to be operating at steady-state conditions, the gimbal function timer was started manually. Generally, all gimbaling programs were limited to a 40-second duration.

#### RESULTS AND DISCUSSION

The results of the investigation are described in the following order: (1) The coulomb and viscous friction of the gimbal pin and other constants necessary for a complete evaluation of the system are presented and discussed, (2) the transient and frequency response data of the system are presented, and (3) the structural integrity of the gimbal system is discussed along with a presentation of the torsional load test information. The procedures used are outlined and the data obtained are presented in tabular and in graphical form. All hot-firing data presented are for rated thrust conditions of 15 000 pounds.

## Determination of Coulomb and Viscous Friction of Gimbal Pin

A complete analysis of the gimbal system requires that constants concerned with the actuators and the facility be determined along with the coulomb and viscous friction of the gimbal pin. Included are the gravitational effects of horizontal mounting of the engine, the thrust offset or misalignment vector, the test-stand flexibility constant, the actuator internal friction, and the facility propellant duct restraints. These constants were obtained as a side result of the coulomb and viscous friction tests or were supplied by the vehicle manufacturer. A summary of the results and the procedures used to obtain them are presented.

Gravitational effects. - The gravitational effects due to horizontal mounting of the engine were determined by noting the actuator differential pressure required to hold the engine at the null position when the propellant ducts were not connected. In the yaw mode, the vehicle manufacturer considered this effect to be negligible or equal to zero; however, a yaw actuator differential pressure of approximately 11 pounds per square inch (actuator extending) was required to maintain a null position. Multiplication of this value (in pounds per square foot) by the actuator piston area (0.0106 sq ft) and the actuator moment arm about the gimbal pin (1.16 ft) yielded a gravitational effect moment value. Since the reaction in the actuator tended to extend the actuator (a positive moment), it can be concluded that the yaw mode gravitational force opposed extension of the actuator to yield a negative moment of 19.5 foot-pounds. The engine offset center of gravity, created by the location of the turbopump package, could possibly have caused this load because the engine would have a tendency to pivot about both the gimbal pin and the pitch actuator ground support.

In the pitch mode, an actuator differential pressure of -434 pounds per square inch (actuator retracting) was required to hold the engine at the null position. Converting this reaction to a moment value about the gimbal pin yielded a gravitational effect of 769 foot-pounds (a tendency to extend the actuator), which is in agreement with the product of the engine weight (including the hydraulic pump and instrumentation) and the distance from the center of mass to the gimbal pin.

The axial location of the engine center of mass would be dependent on the cosine function of the angular displacement. Since the angular displacement was limited in this program to  $\pm 2^\circ$ , the axial distance could be considered as constant; therefore, the gravitational moment about the gimbal pin would also be constant. The amount of force required by the actuators to hold the engine in a position other than null was found by taking the difference between the actuator differential pressures at this position and at the null position. Retracting the actuator from null to  $-2^\circ$  with a step input resulted in an actuator differential pressure of -464 pounds per square inch, and extending the actuator from null to  $2^\circ$  yielded a value of -408 pounds per square inch. In order to hold the engine at  $-2^\circ$  (retracting the actuator), an additional force of 45.8 pounds was thus required. The additional force was due to the fact that the actuator moment arm was shortened, as can be seen in the schematic diagram of the pitch actuator positions in figure 4. A displacement from null to  $2^\circ$  (ex-

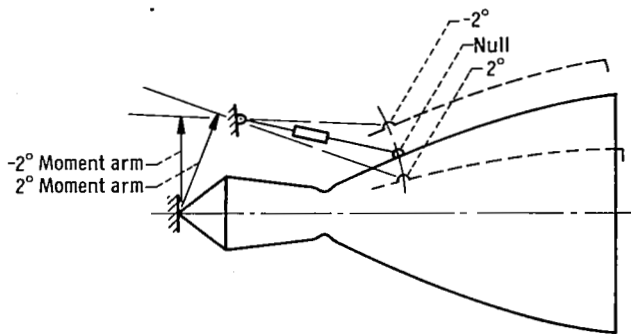


Figure 4. - Pitch actuator positions.

same as for actuator movements; that is, a positive moment tends to extend the actuator, while a negative moment tends to retract the actuator.

The moments due to the engine thrust offset vector  $T_e$  were determined by noting the difference in the actuator differential pressures for firing and nonfiring conditions at the null position. Nonfiring values were obtained after a pressurized engine cool-down period to ensure that ducting forces would be stable, and firing values were taken after the engine reached rated conditions. It was felt that additional duct restraints due to propellant flow would not change appreciably during the intervening start transient. Components of the thrust offset vector were -84 foot-pounds for the yaw mode and -86.5 foot-pounds for the pitch mode.

The method used in determining the facility propellant duct restraints  $C_1$  is presented and discussed later in this section. From a previously described test, the gravitational effects of horizontal mounting  $C_2$  were -19.5 foot-pounds for the yaw mode and 769 foot-pounds for pitch-mode operation. Since the test stand was rigid and had a spring constant several times that of the Centaur vehicle, the flexibility constant  $C_3$  may be neglected. The value of the actuator friction constant  $C_4$ , which was supplied by the vehicle manufacturer, was 18 foot-pounds and would oppose actuator movement.

The coulomb and viscous friction tests were conducted by operating the gimbal system over constant velocity ramps with  $\pm 2^\circ$  excursions and angular velocities of  $1/2^\circ$ ,  $1^\circ$ ,  $2^\circ$ ,  $4^\circ$ , and  $8^\circ$  per second. Presented in figure 5 is the change in actuator differential pressure required to overcome the coulomb and viscous friction as a function of the angular velocity. The data were obtained by noting the difference between the null-position actuator differential pressures for dynamic and static conditions. This procedure was used for movements from positive displacement to null (retraction) and negative displacement to null (extension). Represented on the figure, therefore, is the graphical form of equation (A2) in the appendix when the constant  $K$  ( $K = T_e + C_1 + C_2 + C_3$ ) is equal to zero. Shown are data for both yaw and pitch modes.

Extrapolating the slope of the lines shown in figure 5 to an angular velocity of zero yields an intercept value which will be the coulomb friction plus the actuator friction constant  $B_c + C_4$ . Subtracting the actuator friction

tending the actuator), however, required a force of 39.7 pounds less than that to hold the engine at null because the actuator moment arm was increased.

Results of coulomb and viscous friction tests. - The coulomb and viscous friction terms are presented and defined along with a total system moment balance equation in the appendix. Constants presented are in terms of moments in foot-pounds about the gimbal pin. The sign notation is the

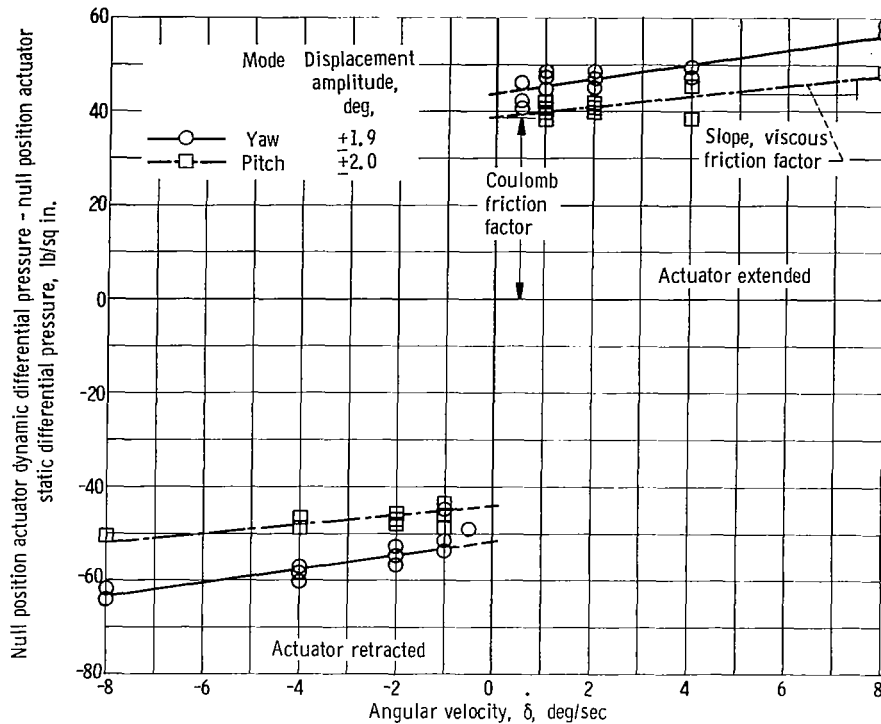


Figure 5. - Difference between null-position actuator differential pressures for dynamic and static conditions as function of angular velocity. Coulomb and viscous friction factors under thrust load noted.

value, the coulomb or constant friction values for the gimbal pin were 66.8 foot-pounds in the yaw mode and 55.3 foot-pounds for the pitch mode.

The viscous or velocity friction was found by obtaining the slope of the lines shown in figure 5. As can be seen, the slopes were approximately the same for extension and retraction; however, the values differed slightly for the yaw and the pitch modes. The slope for the yaw mode was approximately 1.5 pounds per square inch per degree per second, whereas, the pitch-mode value was 1.0 pound per square inch per degree per second. When these values were used, the resulting viscous friction constants for the gimbal pin were 2.66 and 1.77 foot-pounds per degree per second for the yaw and the pitch modes, respectively.

Facility propellant duct restraints. - Experimental determination of the facility propellant duct restraints required a comparison of the actuator differential pressures for engine movements with and without the ducts connected. These tests would be nonfiring and with relatively slow movements; therefore, the coulomb and the viscous friction terms would be negligible. In order to simulate hot-firing conditions, rated propellant flow (approx. 36 lb/sec) would be required to the pump inlets and out through the atmospheric vents shown in figure 1(a)(p. 3). Since there were no adequate means for disposing of the unburned propellants in such quantity, the duct restraint tests were not performed for dynamic conditions.

The method used to determine the facility propellant duct restraints was to substitute the friction terms and constants obtained experimentally (summa-

TABLE II. - SUMMARY OF EXPERIMENTAL CONSTANTS IN  
TERMS OF MOMENTS ABOUT GIMBAL PIN

Constant	Moments <sup>a</sup> about gimbal pin, ft-lb			
	Yaw mode		Pitch mode	
	Extension	Retraction	Extension	Retraction
Coulomb friction, $B_c$	-66.8	66.8	-55.3	55.3
Viscous friction, $B_r$	<sup>b</sup> -2.66	<sup>b</sup> 2.66	<sup>b</sup> -1.77	<sup>b</sup> 1.77
Gravitational effect, $C_2$	-19.5	-19.5	769	769
Flexibility constant, $C_3$	0	0	0	0
Actuator friction, $C_4$	-18.0	18.0	-18.0	18.0
Thrust offset vector, $T_c$	-84.0	-84.0	-86.5	-86.5

<sup>a</sup> Positive moments tend to extend actuator; negative moments tend to retract actuator.

<sup>b</sup> Viscous friction in terms of ft-lb/(deg/sec).

rized in table II) into equation (A2). Resulting values for the yaw mode were 140 foot-pounds when the actuator was retracted and 82 foot-pounds when it was extended, whereas, for the pitch mode, the duct restraint values were 212 and 20 foot-pounds for retraction and extension, respectively.

#### Transient and Frequency Response

As major objectives of the investigation, the transient and the frequency response of the gimbal system were determined. Included are the frequency response parameters (gain and phase lag), the damping characteristic of the gimbal system, and the evaluation of times for 63.2 and 90 percent of change for a step input.

Frequency response of gimbal system. - Tests to determine the frequency response of the gimbal system were conducted by operating the engine over sinusoidal wave input frequencies of 1/4, 1/2, 1, 2, 4, and 8 cps. Nominal amplitude variations included  $\pm \frac{1}{8}^\circ$ ,  $\pm \frac{1}{2}^\circ$ ,  $\pm 1^\circ$ , and  $1 \frac{1}{2}^\circ$  for the yaw mode and  $\pm 1/8^\circ$  and  $\pm 1/2^\circ$  for the pitch mode.

The hot-firing frequency response parameters for the various amplitudes are presented for both operating modes in figure 6. Shown on the figure as a function of frequency are the ratios of engine angular position  $\delta$  measured at the gimbal pin (feedback transducer) to the input demand angular position and the phase lag between these variables. Examination of the data shows that, for both operating modes, the frequency response of the gimbal system was relatively flat to about 0.5 cps. A trend is noted toward greater attenuations with increasing displacements, which is typical for systems such as this; however, the spread is slight.

Presented in figure 7 are the ratios of the engine angular position meas-

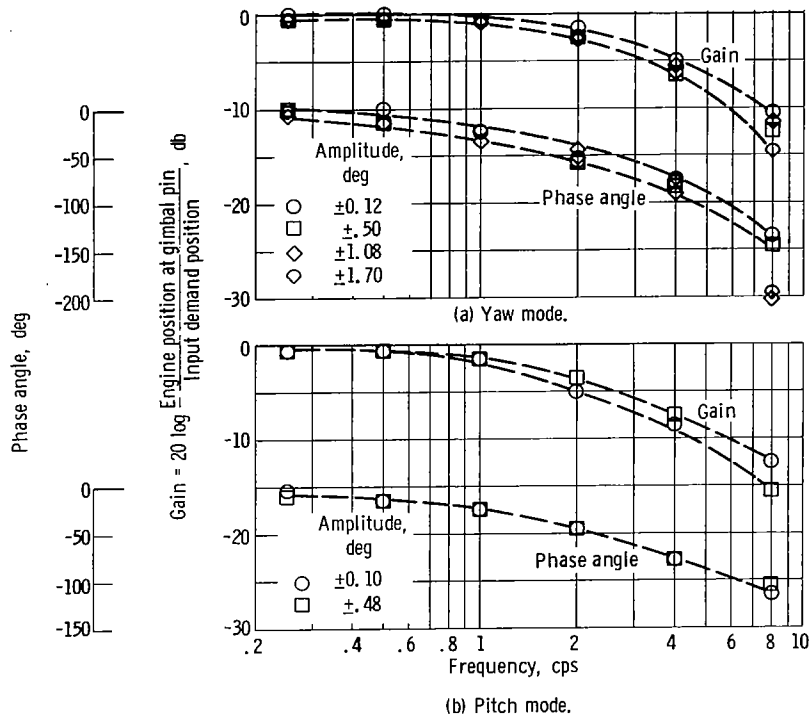


Figure 6. - Hot-firing gimbal system frequency response parameters.

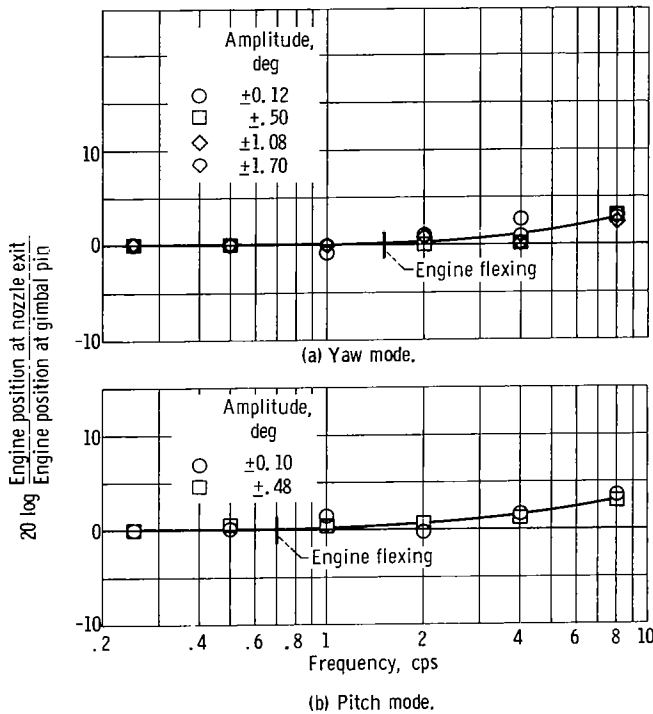


Figure 7. - Comparison of engine position measured at nozzle exit and at gimbal pin for yaw and pitch modes.

ured at the nozzle exit to the engine angular position at the gimbal pin for both operating modes. These data are included to show that flexing of the engine occurred as it was driven at the higher frequencies. Examination of the figure yields that, in the yaw mode, the engine began to flex at approximately 1.5 cps, whereas, the pitch mode, flexing began at about 0.7 cps.

These frequency response data were obtained with the existing facility thrust stand and engine mounts, which had a spring constant several times that of the Centaur vehicle; thus, corrections to the data are necessary for application to softer mounts.

Transient response of the gimbal system. - Determination of the transient response and damping characteristics of the gimbal system were included in the investigation. These

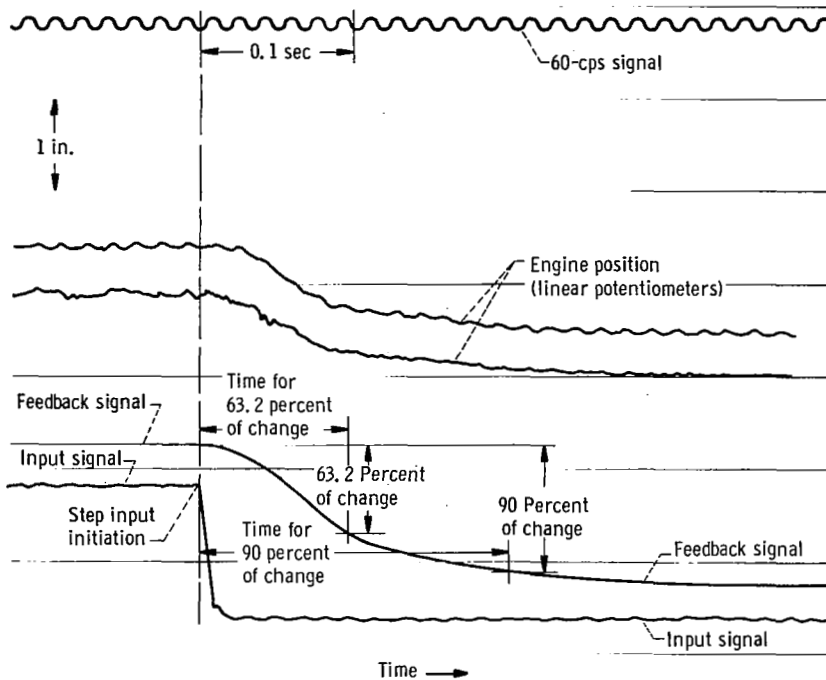


Figure 8. - Copy of typical hot-firing transient response oscillograph trace showing gimbal movement from null position to  $-1^\circ$  (actuator retracted) in yaw mode. Calibration: input signal, 0.695 degree per inch; feedback signal, 0.695 degree per inch; engine positions, 1.0 degree per inch.

TABLE III. - GIMBAL SYSTEM RESPONSE TIMES

	Response time, sec, for -			
	63.2 percent of change		90 percent of change	
	Retraction	Extension	Retraction	Extension
Yaw mode				
Firing	0.093	0.093	0.194	0.194
Nonfiring	.093	.093	.198	.198
Pitch mode				
Firing	0.131	0.080	0.258	0.167
Nonfiring	.135	.085	.273	.167

determinations were obtained by operating the system with step inputs of  $\pm 1/4^\circ$ ,  $\pm 1/2^\circ$ , and  $\pm 1^\circ$  displacement about the null position.

Examination of the feedback signal trace, shown in a copy of a typical oscillograph record presented in figure 8, shows that the gimbal system response was nonoscillatory and generally similar to an overdamped second-order system. Response times for the system may be measured, for a step input, as time to 63.2 and 90 percent of change as noted in figure 8. Since the response times for the range

of displacements tested were within a 0.02-second band, average values for the various operating modes are presented in table III.

As can be seen from the data presented in table III, the yaw mode response times for firing and nonfiring compared favorably. The difference between the pitch mode response times for retracting the actuator (up) and extending the actuator (down) was caused by the gravitational effect of mounting the engine

horizontally. No appreciable difference was noted in the yaw mode response times for firing and nonfiring when retracting or extending; however, one can be seen for the pitch mode response times for firing and nonfiring when retracting the actuator. The response time for firing is less than that for nonfiring, which can be explained by the direction of the thrust offset or misalignment vector, which has components, viewed upstream, that are up and to the right. The vertical component of this force tends to help upward movements and retard downward movements. The values of the thrust offset vector components are listed in table II (p. 11).

#### Demonstration of Structural Integrity of Gimbal System

One of the major objectives of the investigation reported herein was to demonstrate the structural integrity of the engine and the actuators under dynamic stresses. Presented throughout this report are data obtained from a variety of tests designed to meet this objective. Among these was the evaluation of factors concerned with the torsional loads on the gimbal pins created by the off-center location of the center of mass of the engine. These factors were determined for slow movements, step changes, and for cycling operation.

Torsional load tests. - Consideration was given to the torsional load effect created by the location of the engine turbopump. As can be seen in figure 9, the center of mass of the engine is located off the axial centerline and, thus, rapid engine movements would create a torsional load on the gimbal pin. In order to measure this force, a collar which was free to rotate was mounted in place of the standard thrust load cell. An arm extending from the collar was connected to a load cell, as shown in figure 10, and yielded a torsional load measurement. The engine was slowly displaced to the actuator limits and then, with a step input, was returned to the null position. Operation was limited to the yaw mode because of the possibility of exceeding the load limits of the pitch actuator.

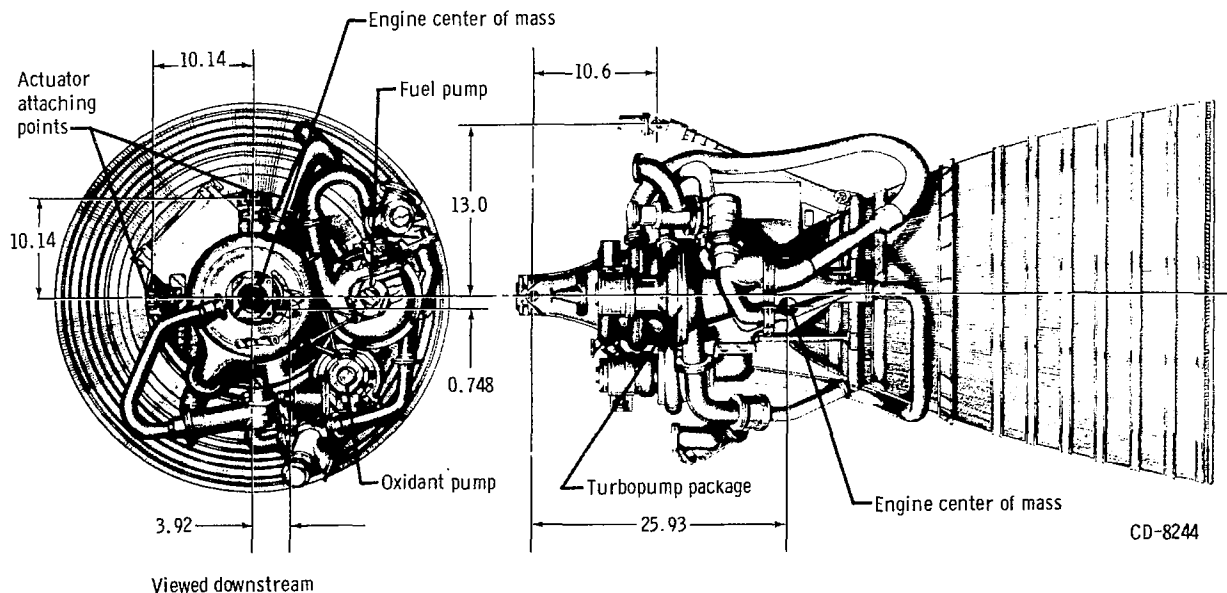


Figure 9. - Engine schematic diagram showing location of center of mass.

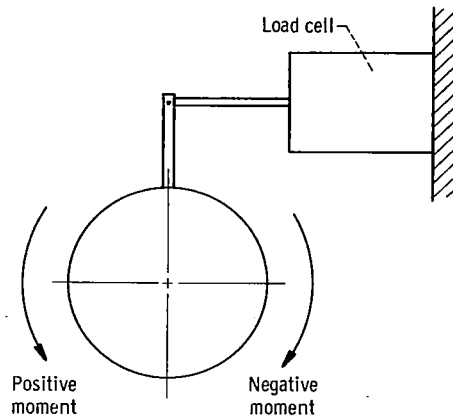
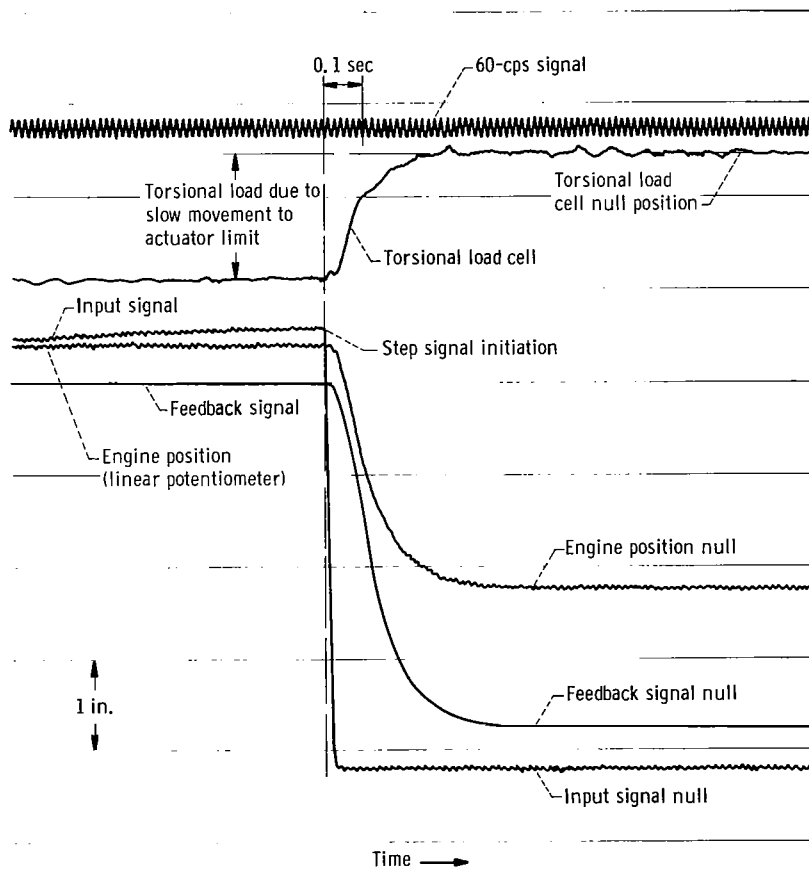
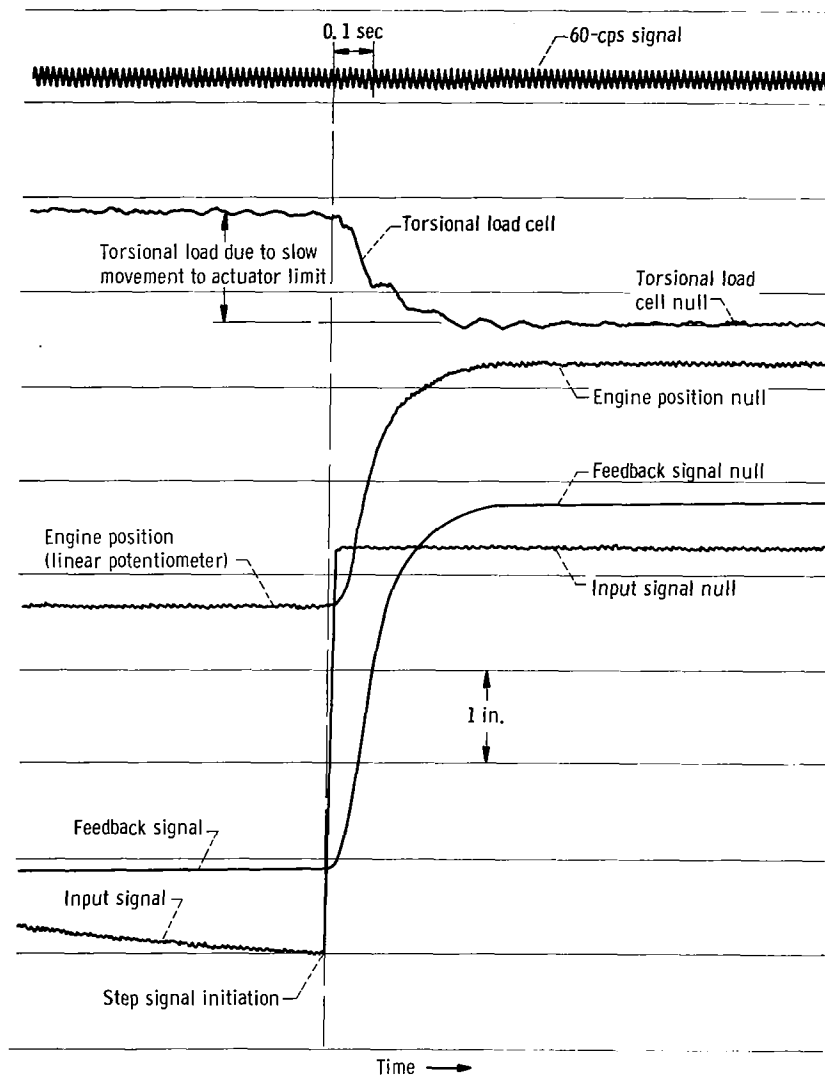


Figure 10. - Torsional load measurement apparatus (viewed upstream).



(a) Step change from positive limit (actuator extended) to null.

Figure 11. - Typical hot-firing oscillograph record showing torsional load cell response to step change. Calibration: torsional load, 125 foot-pounds per inch; input signal, 0.667 degree per inch; feedback signal, 0.671 degree per inch; engine position, 1.0 degree per inch.



(b) Step change from negative limit (actuator retracted) to null.

Figure II. - Concluded.

When the engine was slowly displaced from the null position to the actuator limits (approx.  $2\frac{1}{2}^{\circ}$ ), a dynamic torsional load, in addition to one created by the offset center of gravity of the engine, was noticed at the gimbal block. This load can be seen on the copies of typical oscillograph records presented in figure 11 just prior to the point of step signal initiation. The additional torsional effect can be explained by the fact that the engine does not move laterally but pivots about the pitch actuator ground support and thus creates a torsional moment. When the actuator was extended to its limit, an average additional torsional moment of 155 foot-pounds clockwise (viewed upstream) resulted, whereas, the actuator was retracted, the average additional moment value was found to be 130 foot-pounds counterclockwise.

The engine was then returned to the null position with a step input signal. As can be seen in figure 11, the torsional load created by displacing the engine to the actuator limits was returned to its null value without an overshoot; however, a slight ringing occurred, which amounted to approximately  $\pm 7.5$  foot-pounds. These data indicate that no appreciable dynamic torsional effect will be created by step movements of the engine from the actuator limits to the null position.

Additional dynamic torsional effects during cycling operation were also determined. The system was operated sinusoidally in the yaw mode over frequencies ranging from 1 to 4 cps with an input signal amplitude of  $\pm 1/2^\circ$ . Because of the frequency response of the system, the actual angular displacement varied from  $\pm 0.44^\circ$  to  $\pm 0.24^\circ$  at 1 and 4 cps, respectively. The ratio of the torsional moment to the angular displacement, however, appeared to be constant, with an average value of 77 foot-pounds per degree, which indicated that the moment value was not a function of the operating frequency. For the amplitude range investigated, the additional torsional moment due to cyclic operation could therefore be considered as a linear function of the angular displacement.

Additional demonstrations of structural integrity of the gimbal system. - Described throughout this report are a variety of tests designed to demonstrate the structural integrity of the gimbal system under thrust load. Many of these tests exceeded the loads and requirements of the system as defined for actual flight conditions in unpublished data supplied by the vehicle manufacturer. One such example would be the frequency response tests. During these tests, the system was operated sinusoidally over frequencies from 1/4 to 8 cps with amplitude variations ranging from  $\pm \frac{1}{8}^\circ$  to  $\pm 1\frac{1}{2}^\circ$  for the yaw mode and  $\pm \frac{1}{8}^\circ$  and  $\pm \frac{1}{2}^\circ$  in pitch. The maximum angular velocities tested were therefore  $48^\circ$  per second in yaw and  $16^\circ$  per second in pitch, whereas the system requirements call for maximum angular velocities of  $5^\circ$  and  $8^\circ$  per second for yaw and pitch, respectively. The system was thus concluded to be sound and would meet the vehicle flight requirements.

Throughout the test program, the gimbal system, which includes the engine, the hydraulic system, and the actuators, endured without any hardware failures. The structural integrity of the system was thus demonstrated by the various tests described within this report.

## SUMMARY OF RESULTS

An investigation was conducted to determine the response characteristics of a Centaur gimbal system. The data presented are based on the facility mounting of the engine. The actuator planes were rotated about the engine axial centerline  $90^\circ$  to that of the Centaur vehicle; that is, the facility yaw plane corresponds to the vehicle pitch plane, and the facility pitch plane corresponds to the vehicle yaw plane. A positive moment value indicates a tendency to extend the actuator, whereas a negative moment tends to retract the actuator.

1. The gravitational effects due to horizontal mounting of the engine were determined. These effects are normally considered to be negligible or equal

to zero for yaw-mode operation; however, a moment of 19.5 foot-pounds was required to hold the engine in the null position. In the pitch mode, a moment about the gimbal pin of 769 foot-pounds was needed to hold the engine at the null position. A step change from null to  $-2^{\circ}$  (actuator retracted) required an additional force of 45.8 pounds, while a movement from null to  $2^{\circ}$  (actuator extended) required a force of 39.7 pounds less than that to hold the engine at the null position.

2. The thrust offset vector coordinates for the engine used for the tests were determined. Moment values about the gimbal pin were -84 foot-pounds for the yaw plane and -86.5 foot-pounds for the pitch plane.

3. Coulomb and viscous friction values of the gimbal pins were determined. The coulomb or constant-friction values were 66.8 foot-pounds for the yaw mode and 55.3 foot-pounds for the pitch mode. The viscous or velocity-friction values were 2.66 and 1.77 foot-pounds per degree per second for the yaw and the pitch modes, respectively.

4. The facility propellant duct restraints were found for actuator retraction and extension for both yaw and pitch modes. In the yaw mode, the resulting duct restraint moments were 140 foot-pounds for retraction and 82 foot-pounds for extension. The pitch mode values were 212 and 20 foot-pounds for retraction and extension, respectively.

5. The frequency response of the system was flat to 0.5 cps for both yaw and pitch modes with a trend for greater attenuations with increasing angular displacements. Flexing of the engine was noted at approximately 1.5 cps for yaw-mode operation and at about 0.7 cps in pitch.

6. The gimbal system was nonoscillatory and generally similar to an overdamped second-order system.

7. System response times for a step input were found for both 63.2 and 90 percent of change in both yaw and pitch modes. In the yaw mode, for hot-firing conditions, the response time for 63.2 percent of change was 0.093 second, while the time for 90 percent of change was 0.194 second. The hot-firing response times in the pitch mode varied, depending on whether the actuator was extended or retracted. For actuator extension, the response times were 0.080 second for 63.2 percent of change and 0.167 second for 90 percent of change, whereas for retraction, the response time values were 0.131 second and 0.258 second for 63.2 and 90 percent of change, respectively.

8. When the engine was slowly displaced from the null position in the yaw mode, a torsional moment, in addition to one created by the location of the engine center of mass, was observed. The additional moment values ranged from 155 foot-pounds for actuator extension to 130 foot-pounds for retraction.

9. A step change from the actuator limits  $\left(\text{approx. } \pm 2\frac{1}{2}^{\circ}\right)$  to the null position produced a slight ringing in the torsional load cell, amounting to  $\pm 7.5$  foot-pounds, without an overshoot.

10. The torsional moment effect of sinusoidal cycling of the system could be considered as a linear function of the angular displacement. Resulting ratios of the torsional moment to the angular displacement appeared to be a constant of approximately 77 foot-pounds per degree.

11. The structural integrity of the gimbal system under thrust was demonstrated in the various tests performed and described herein.

Lewis Research Center,  
National Aeronautics and Space Administration,  
Cleveland, Ohio, October 6, 1965.

APPENDIX - DEFINITION OF COULOMB AND VISCOUS FRICTION TERMS

The method of calculating the coulomb  $B_c$  and viscous  $B_r$  friction values are defined as follows:

A biaxial summation of the total system moments about the gimbal pin for the null position yields the following equation:

$$AR \Delta P = \frac{I_r \ddot{\delta}}{57.3} + B_r \dot{\delta} + B_c \frac{\dot{\delta}}{|\dot{\delta}|} + T_\epsilon \pm C_1 \pm C_2 \pm C_3 \pm C_4 \quad (A1)$$

where

A	actuator piston area, sq ft
R	actuator moment arm, ft
$\Delta P$	actuator differential pressure, lb/sq ft
$I_r$	engine mass moment of inertia, slug-sq ft
$\dot{\delta}$	angular velocity, deg/sec
$\ddot{\delta}$	angular acceleration, deg/sec <sup>2</sup>
57.3	conversion constant, deg/rad
$B_r$	viscous friction, ft-lb/(deg/sec)
$B_c$	coulomb friction, ft-lb
$T_\epsilon$	thrust offset vector, ft-lb
$C_1$	duct restraints, ft-lb
$C_2$	gravitational effects, ft-lb
$C_3$	flexibility constant, ft-lb
$C_4$	actuator internal friction, ft-lb

If the angular velocity  $\dot{\delta}$  is constant, the angular acceleration  $\ddot{\delta}$  would equal zero; the inertial term would thus be eliminated. If  $K = T_\epsilon + C_1 + C_2 + C_3$ , equation (A1) becomes

$$AR \Delta P = B_r \dot{\delta} + B_c \frac{\dot{\delta}}{|\dot{\delta}|} \pm K \pm C_4 \quad (A2)$$

which is the equation for a straight line in intercept form. Presented in figure 12 is equation (A2) for extension and retraction of the gimbal system actu-

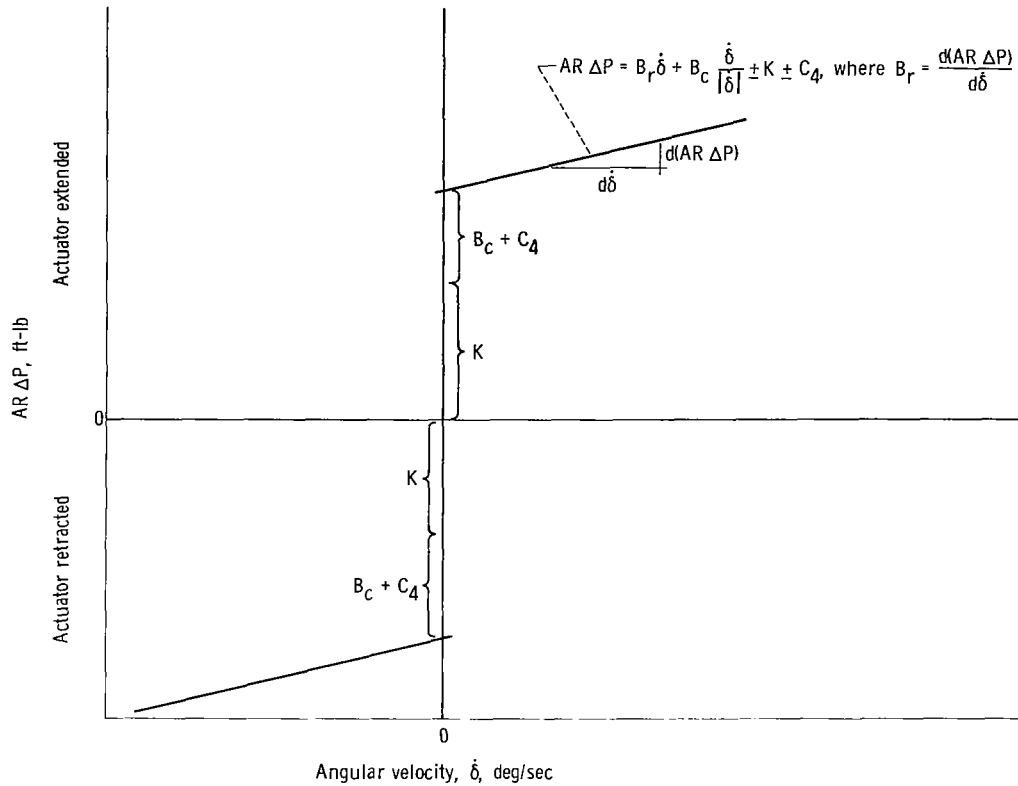


Figure 12. - Graphical presentation of equation (A2) for extension and retraction of gimbal system actuators.

ators. When the angular velocity  $\dot{\delta}$  is equal to zero, the coulomb or constant friction  $B_c$  can be defined as the average differential pressure intercept minus  $K + C_4$ . The viscous or velocity friction  $B_r$  can be defined as the average slope of the lines for extension and retraction.

Equations (A1) and (A2) as shown are precise for the null position; however, other terms should be added if they are to be used for any other angular position. Such terms as the torque at the gimbal pin and at the actuator mounts would have to be included, because the engine does not move laterally (yaw) or vertically (pitch) but pivots on the actuator ground supports.

## REFERENCES

1. Wanhainen, John P.; Antl, Robert J.; Hannum, Ned P.; and Mansour, Ali H.: Throttling Characteristics of a Hydrogen-Oxygen, Regeneratively Cooled, Pump-Fed Rocket Engine. NASA TM X-1043, 1964.
2. Conrad, E. William.; Hannum, Ned P.; and Bloomer, Harry E.: Photographic Study of Liquid-Oxygen Boiling and Gas Injection in the Injector of a Chugging Rocket Engine. NASA TM X-948, 1964.
3. Bloomer, Harry E.; Renas, Paul E.; and Antl, Robert J.: Experimental Investigation in an Altitude Test Facility of Burning of Excess Combustibles in a Rocket Engine Exhaust. NASA TN D-200, 1960.
4. Anon.: RLLOA-3 Liquid Rocket Engines Service Manual. Pratt & Whitney Aircraft, Aug. 15, 1962.
5. Anon.: RLLOA-3 Liquid Rocket Engines Installation Manual. Pratt & Whitney Aircraft, 1961.
6. Davis, Howard D.: The Centaur Hydraulic System. Paper Presented at Vickers Aerospace Fluid Power Conf., Detroit (Mich.), Apr. 29-30, 1962.
7. Ladd, John W.: A Durable and Reliable Test Stand System for High-Accuracy Temperature Measurements in the Cryogenic Ranges of Liquid Hydrogen and Liquid Oxygen. Vol. VI of Advances in Cryogenic Eng., K. D. Timmerhaus, ed., Plenum Press, 1961, pp. 388-395.